POLITECNICO DI TORINO
Repository ISTITUZIONALE

GSTOP: a new tool for 3D Gemophogical survey and mapping

(Article begins on next page)

25 April 2024
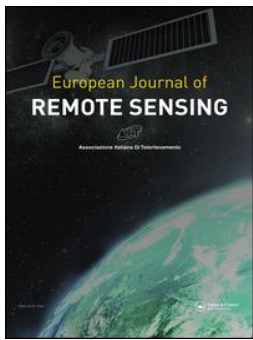
GSTOP: a new tool for 3D geomorphological survey and mapping

Gabriella M. Forno, Andrea M. Lingua, Stefano Lo Russo, Glenda Taddia & Marco Piras

GSTOP: a new tool for
3D geomorphological survey and mapping

Gabriella M. Forno[1], Andrea M. Lingua[2*], Stefano Lo Russo[2],
Glenda Taddia[2] and Marco Piras[2]

[1]Università degli Studi di Torino, Department of Earth Sciences,
Via Valperga Caluso 35, 10125 Torino, Italy
[2]Politecnico di Torino, Dipartimento di Ingegneria dell'Ambiente, del Territorio e delle Infrastrutture
(DIATI), C.so Duca degli Abruzzi 24, 10129 Torino, Italy
*Corresponding author, e-mail address: andrea.lingua@polito.it

Abstract

In geological mapping activities, geomatics can facilitate data collection during field survey and avoid practical problems related to the transposition of these data onto maps for GIS production. The Solid True Orthophoto (STOP) can reduce these difficulties using a dedicated instrument developed by the Authors called GSTOP. It can run on laptops or tablets, managing a direct connection with low cost navigation sensors in real time, to define its location and attitude. The user can produce a 3D solid image in order to compare the effective scene to record notes and to acquire evidence. GSTOP has been used to produce a geomorphological map of the Rodoretto Valley (Germanasca Valley, NW Italy), reconstructing its Quaternary evolution.

Keywords: Geomorphological survey, solid true orthophoto, in field data acquisition, quaternary map.

Introduction

Geological mapping is an interpretive process involving multiple types of information, from analytical data to subjective observations, collected and synthesised by a researcher. With field experience, geologists generally develop effective personal styles of relatively efficient mapping. This "traditional" geological mapping can be accomplished by a geologist almost as effectively in inclement weather and when surrounded by mosquitoes as in ideal conditions [Athey et al., 2008]. Each geologic map, regardless of scale, requires a certain level of field mapping, where data are recorded on a topographic plot, on aerial photographs and in a field book. Traditionally, geological elements are hand-transferred to a topographic base, on which the final map is prepared for publication using known cartographic techniques [Brown and Sprinkel, 2008].

234

Digital Geological Mapping (DGM) is the process of collecting and mapping geological data using some form of portable computer and Global Navigation Satellite System (GNSS), rather than a traditional approach based on notebook and paper map [McCaffrey et al., 2005]. Digital mapping is rapidly becoming accepted and established as a valuable tool for geoscientists. Recently, numerous papers have discussed the methodology, software development, applications and merits of DGM [Jones at al., 2004; Wilson et al., 2005; Clegg et al., 2006]. Many geoscientists have used a palm-sized Personal Digital Assistant (PDA) or similar device and customised software applications [Brodaric, 1997; Walsh et al., 1999; Brimhall et al., 2002; Edmondo, 2002]. Furthermore, other researchers have chosen systems based on larger rugged tablet computers [De Donatis et al., 2005; Sprinkel and Brown, 2008] that offer the following distinct advantages despite its encumbrance [Brown and Sprinkel, 2008]:

1) improved precision in placement of geologic features and outcrop location using Global Navigation Satellite System (GNSS) and on-screen display of geospatially corrected imagery and topographic base of reference;

2) increased efficiency in drawing field-attributed geologic lines because they do not need to be hand-transferred or redrawn on another map in the office and then digitised;

3) possibility of graphical notation on digital photographs with geological data;

4) opportunity to access key publications in a digital library.

These papers document the ongoing technological development that has allowed the relatively unwieldy computer equipment that was available to the early digital pioneers, to be replaced by lightweight and user-friendly DGM systems. Most modern users favour a DGM setup based around a palm-sized Personal Digital Assistant (PDA) or a larger Tablet PC.

The actual DGM systems expose some limits due to the lack of 3D visualisation and collection. In fact, the basic data of commercial DGM is a 2D map or an orthophoto, which constitutes the reference coordinate system for data recording and visualisation. Despite using GNSS and a compass, the user has difficulty in correctly locating the information because he must compare what he sees (a natural 3D perspective view) with a 2D mapping data (some contour lines, mapping details, orthophotos, etc.). Moreover, the acquired data are located using the GNSS position, which has a metrical level of accuracy in stand-alone method. This position has to be considered less than accurate for 3D positions due to GNSS precision, ellipsoidal height and others aspects.

To fill these gaps, the authors propose the use of a Solid (True) OrthoPhoto (STOP) [Dequal and Lingua, 2003], which provides a complete 3D land data set [De Agostino et al., 2012] and correct aerial photographic information in a geo-referenced form directly on-site during the survey [Forno et al., 2011].

The Solid True OrthoPhoto (STOP)
Definition
A digital orthophoto is a geometrically corrected photographic representation of a territory. It has the same accuracy as a traditional topographic map [Kraus, 1997] but contains much more information, such as aerial photographic details.

Whether natural or manually modified, a territory is realistically represented without the codes or the symbology used in a digital map production. Each pixel of an aerial image is orthogonally projected onto a cartographic plane, producing a geometrically correct map. The orthophoto functions like a traditional map; angles, distances and coordinates can be read

and measured. While the correct interpretation of a digital map requires technical training, an unskilled user, to a basic easy level, can correctly read and interpret an orthophoto.

Orthophotos may be employed in land-planning applications such as infrastructural planning, land-use monitoring and geological mapping. In fact, through the use of orthophotos, it is possible to recognise and interpret several geological details in 2D [Barnes and Lisle, 2004] clearly detectable at different viewing scales.

Adding 3D information by means of a dense digital surface model (DSM), it is possible to enhance the quality of the geomorphological information surveyed, to optimise the understanding of the geo-phenomena and their evolution. However, difficulties may be encountered where the land surface is characterised by discontinuities and hidden areas. In these situations, commercially available software may be ineffective in producing an acceptable orthophoto [Kraus, 1997] and thus, a DDSM, acquired for example, with light detection and ranging (LiDAR) techniques [Dequal and Lingua, 2003; Pirotti et al., 2012], becomes necessary.
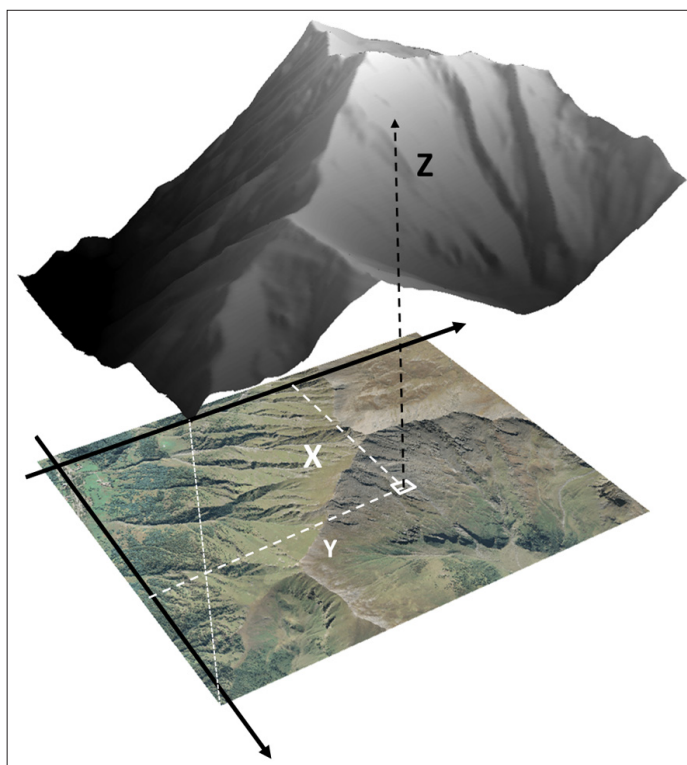

Figure 1 -The schema of STOP.

A true orthophoto can be displayed, analysed and queued in a georeferenced manner using GIS software. The height values derived from the DDSM can be merged with the orthophoto to create the STOP. As shown in the schema of Figure 1, the result is a correct 3D location of the coloured pixels of the true orthophoto.

The structure of STOP

The STOP is a set of various matrices with the same pixel size, number of rows and number of columns. Thus, it is possible to record for each pixel of a STOP (Fig. 2):

1) one height value derived from the DDSM and recorded as a short integer (C variable type, 2 bytes/pixel can represent a value between -327.67 and +327.68 m) or a float (C variable type for single precision, 4 bytes/pixel, 32 bit/pixel, which can represent any possible value);

2) three colour values (Red, Green and Blue, RGB) related to colour image extracted from the orthophoto (3 bytes/pixel);

3) additional matrices that contain other radiometric data as nearest, medium or thermal infrared, multispectral or hyperspectral bands (1 bytes/pixel for each band).
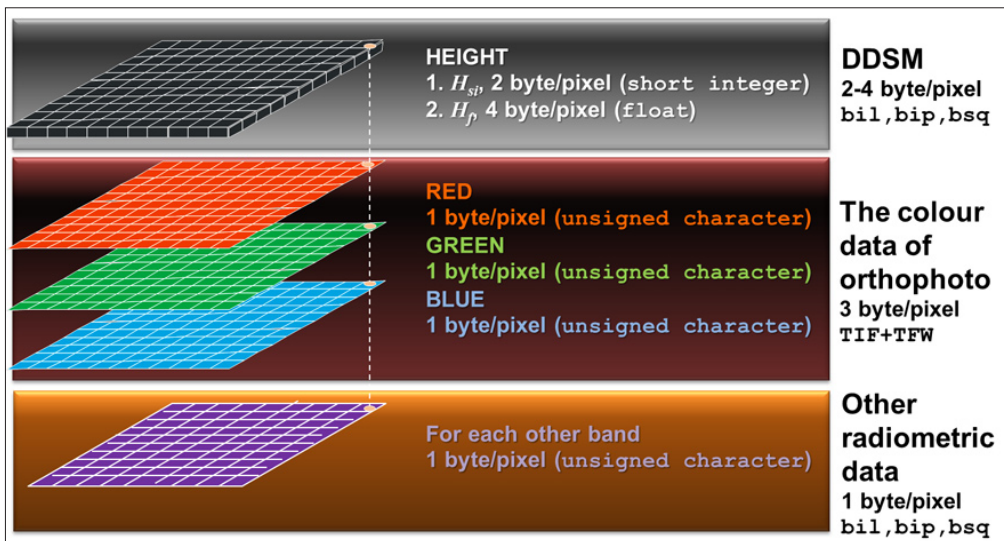

Figure 2 - The structure of STOP.

The viewer of STOP

An experimental software tool has been developed in Visual Fortran (with GINO and GINOMENU graphic libraries, version 7.5) to manage the STOP application. This user interface includes simple query functions, zoom and pan features, a 3D coordinate viewer and some measurement tools (e.g., angles, 3D distances, areas, volumes). These features are useful during geomorphological field surveys. As shown in Figure 3, specific commands prompt STOP to: (a) measure 3D distances and angles; (b) determine areas; (c) directly calculate (with a least squares procedure) and record dip and dip direction of planes using the 3D coordinates of their surface points; (d) extract the intersection between planes and the land surface; (e) define complex volume calculations from the intersection of the topographic surface with several planes.

When STOP is uploaded on a tablet PC, the interface will permit the use of an electronic pen to directly map geomorphological features in the field. Thus, STOP replaces the traditional topographic map.

Recently, a newly incorporated feature permits an ODBC connection to a simple GeoDataBase for directly recording data in a structured way in the field.
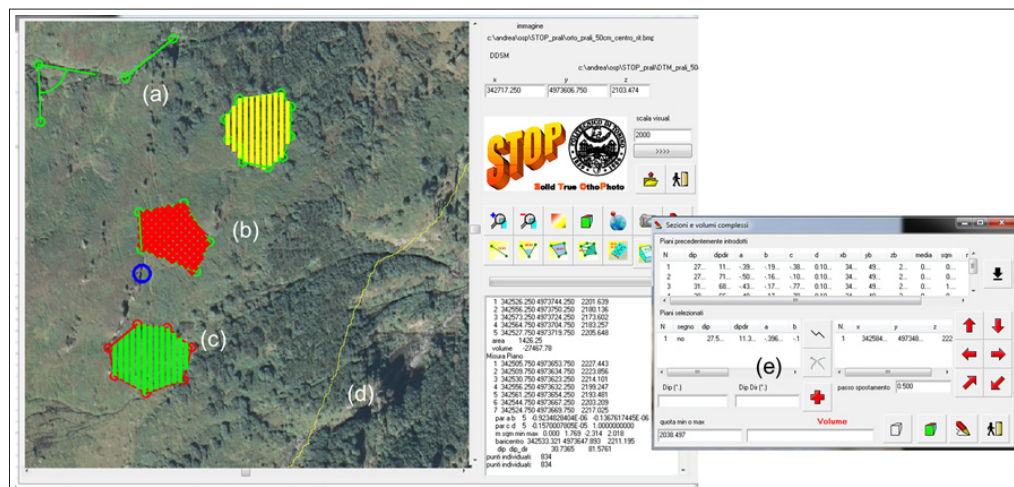

Figure 3 - The main functions of STOP viewer.

The GNSS Solid True OrthoPhoto (GSTOP)

The STOP viewer has been recently improved by the inclusion of some new features based on connectivity with low cost navigation sensors. These devices (Fig. 4) have been derived from Mikrokopter units developed from an Unmanned Aerial Vehicle: MK-Navictrl (CPU), MK3mag (3-axis magnetic field sensor as a low cost Inertial Measure Unit, IMU), MKGPS (based on the LEA-6S receiver chipset by Ublox) and MKUSB/XBee wireless link to the PC.
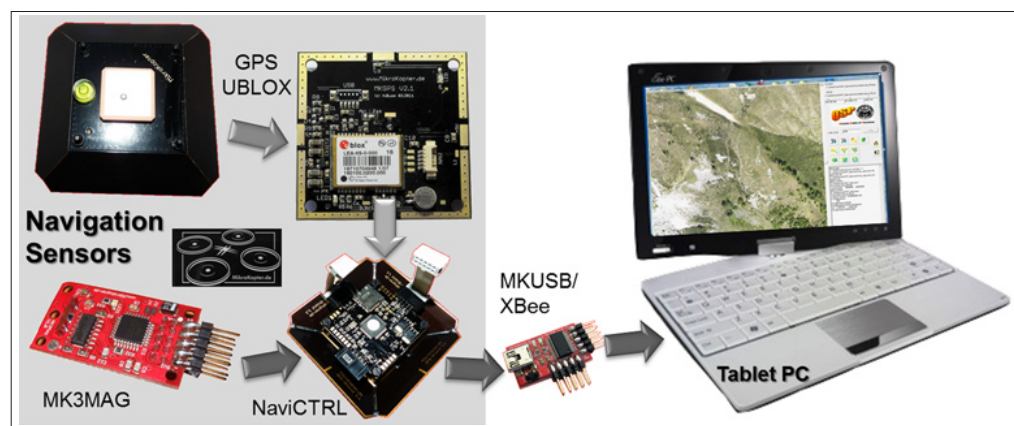

Figure 4 - The navigation sensors of GSTOP.

The integrated portable GNSS (with Hybrid GPS/SBAS engine for WAAS, EGNOS, MSAS) determines the surveyor's position in the mapping coordinate system (X_0, Y_0, Z_0) and a low cost IMU measures the attitude angles (ω, ϕ, κ) of the Tablet PC with respect to (X, Y, Z), as shown in Figure 5. This information can be displayed in real time in the STOP viewer using a circle (user's position) and a red arrow (horizontal direction of his point of view).

Furthermore, the navigation data are useful for generating a natural 3D perspective view, similar to that which the user sees, in order to assist and improve the geological detail collection; this product is a Solid Image (SI) defined below [Bornaz and Dequal, 2003].

The navigation data can also be acquired using other kinds of higher specification GNSS/IMU sensors, in order to obtain data that are more precise.
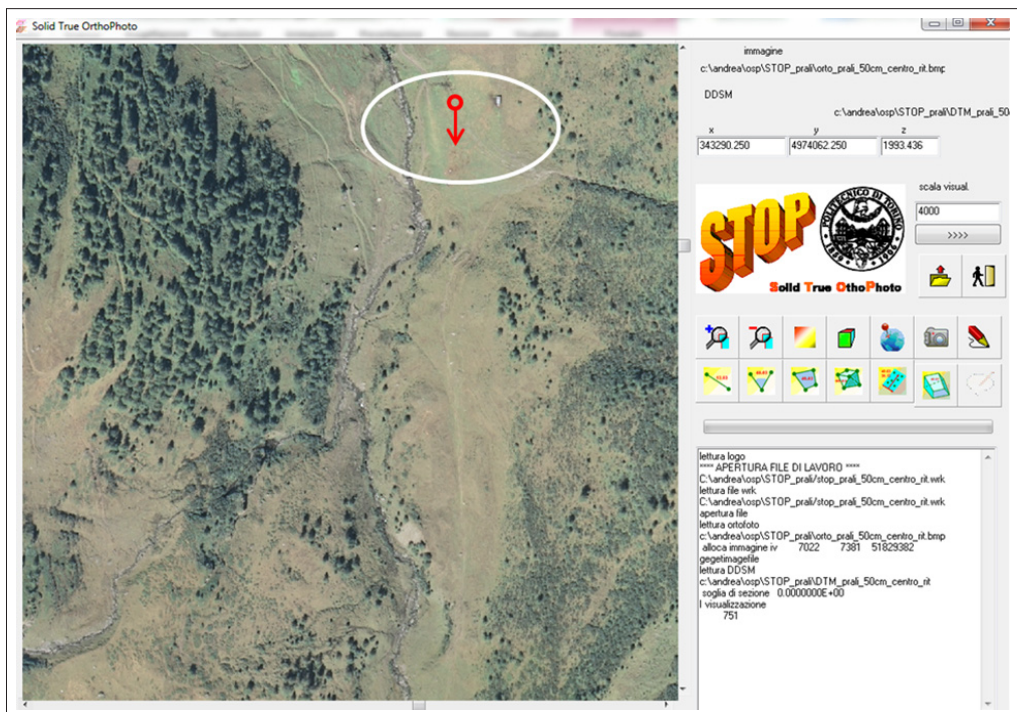
Figure 5 - The main view of GSTOP.

Definition of Solid Image

To a good approximation, any image can be considered as a central perspective of the photographed object. If the internal orientation parameters of the digital camera (position of perspective centre in image coordinate system ζ, η) are known, it is possible to establish a direction (α, θ) in the object coordinate system (x, y, z) for each pixel I of the image (see Fig. 6a) measuring its image coordinates (ζ_I, η_I):

$$\theta = arctan\frac{\xi_I}{c} \qquad \alpha = \frac{\eta_I}{\sqrt{c^2 + \xi_I^2}} \quad [1]$$

where c is the principal distance of the photographic camera that generates the image.
One image is not sufficient to determine the 3D position of an object point. If a single image is used, it is only possible at best, to establish its direction in the space. In order to reconstruct objects in three dimensions, it is necessary to use at least two images according to the classical principles of photogrammetry.
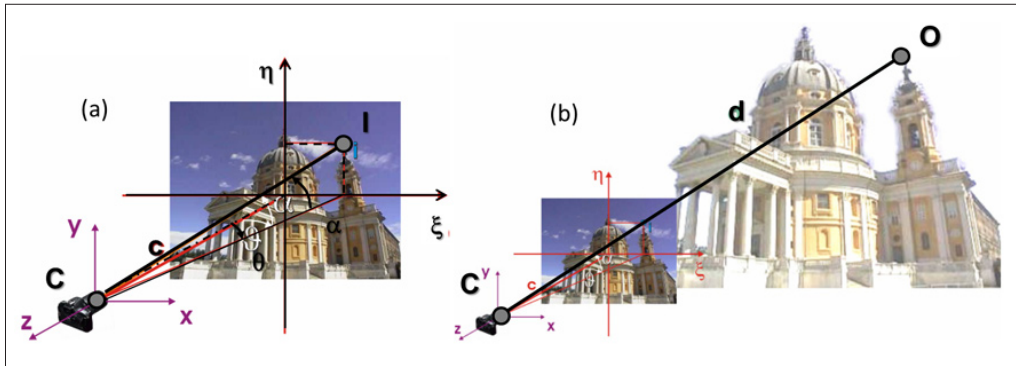

Figure 6 - Definition of Solid Image.

A valid alternative to the well-known photogrammetric restitution techniques is offered by the knowledge of the distance d between the centre of perspective of an image and the object itself for each direction in the space (Fig. 6b). In this way, it is possible to establish the position of any object point O in the (x, y, z) coordinate system, using simple geometric equations:

$$\begin{cases} x_0 = d\ cos\alpha\ sin\theta \\ y_0 = d\ sin\alpha \\ z_0 = -\ d\ cos\alpha\ cos\theta \end{cases} \quad [2]$$

where θ, α are determined as previously shown [1].
The coordinates (x_o, y_o, z_o) can be transformed into the mapping coordinate system (X, Y, Z) by means of a simple 3D roto-translation that can be defined using the navigation data (point of view position and attitude).
The structure of the SI is similar to the STOP; the traditional RGB colour data (and other radiometric band) of the image are completed with a supplementary "range matrix" that has the same size as the RGB matrices, in terms of pixel size, number of rows and columns and contains distance data for each pixel.

Solid Image generation using STOP

In order to generate an SI, the orthophoto and the DDSM contained in a STOP can be used. First, it is necessary to define the characteristics of a "virtual" digital camera that supposedly produced the photographic image: focal length, pixel size, number of rows and columns. The SI matrices can be created and filled with zero values. In this case, the lens distortion and other camera calibration parameters are considered null.

The second step consists of projecting each pixel of the STOP onto the SI. This operation consists in calculating for each pixel of the STOP, the corresponding image coordinates ξ, η using collinearity equations:

$$\xi = -c\frac{r_{11}(X - X_0) + r_{21}(Y - Y_0) + r_{31}(Z - Z_0)}{r_{13}(X - X_0) + r_{23}(Y - Y_0) + r_{33}(Z - Z_0)}$$

$$\eta = -c\frac{r_{12}(X - X_0) + r_{22}(Y - Y_0) + r_{32}(Z - Z_0)}{r_{13}(X - X_0) + r_{23}(Y - Y_0) + r_{33}(Z - Z_0)} \qquad [3]$$

where: (X_0, Y_0, Z_0) are the mapping coordinates of projection centre (GNSS);
(X, Y, Z) are the mapping coordinates of a STOP pixel;
r_{ij} are the 9 elements of a 3×3 rotation matrix defined by (ω, ϕ, κ) (IMU);
c is the focal length;
(ξ, η) are the (solid) image coordinates of a projected STOP pixel.

The distance between the STOP pixel and projection centre can be calculated by:

$$d = \sqrt{(X - X_0)^2 + (Y - Y_0)^2 + (Z - Z_0)^2} \quad [4]$$

The relative pixel of the SI is defined using (ξ, η) and the SI pixel size and then the STOP data (RGB, d and other radiometric data) can be written into the SI matrices in this corresponding position.

The density of the pixels in the digital image is usually much higher than that of the STOP data. For this reason, when the STOP data is projected onto the digital image, the matrices that compose the SI are not completely filled; the distance and the RGB values are only associated to some pixels (this quantity depends on the density of the STOP data and on the image resolution in terms of dpi). In order to fill these gaps, it is necessary to integrate the missing values with an interpolation process. The "inverse distance weighted method" has been used for faster processing [Biasion et al., 2005]. The four nearest pixels, of which the value (distance or RGB values) is known, are considered.

Solid Image generation using additional digital camera and DTM of STOP

If the surveyor uses an additional digital camera, then the SI generation becomes easier.
In fact, the photographic image acquired with the digital camera can be used as the RGB matrices. Therefore, the SI inherits the RGB image from the digital camera that must be calibrated to define:

1) internal orientation parameters: focal length c, image coordinates of principal point (ξ_0, η_0);
2) image sensor characteristics as pixel size, number of rows and columns;
3) lens distortion and sensor calibration $(\Delta\xi, \Delta\eta)$ that give the difference of the real photographic image with respect to ideal perspective [McGlone et al., 2004].

The external orientation parameters X_0, Y_0, Z_0 (GNSS receiver) and ω, ϕ, κ (IMU) can be determinate supposing that the camera is one with the Tablet PC.

In order to define the range matrix of the SI, the DDSM of STOP can be used by applying modified collinearity equations:

$$\xi = \xi_0 + \Delta\xi - c\frac{r_{11}(X - X_0) + r_{21}(Y - Y_0) + r_{31}(Z - Z_0)}{r_{13}(X - X_0) + r_{23}(Y - Y_0) + r_{33}(Z - Z_0)}$$
$$\eta = \eta_0 + \Delta\eta - c\frac{r_{12}(X - X_0) + r_{22}(Y - Y_0) + r_{32}(Z - Z_0)}{r_{13}(X - X_0) + r_{23}(Y - Y_0) + r_{33}(Z - Z_0)} \quad [5]$$

As described in the previous paragraph, the range matrix is not completely filled; it is necessary to integrate the missing values with an interpolation process using the "inverse distance weighted method". The four nearest pixels, of which the distance value is known, are considered.

The Solid Image viewer included in GSTOP

An example of the SI generated in this way is shown on the right side of Figure 7 (SI).

The surveyor observes a 2D perspective image (as a photographic image) similar to what he sees in the field, then he can measure and record the features of some evidences (distance, angle, area, dip, dip direction) in a 3D way using the hidden information of the range matrix. Moreover, the user can acquire points, polylines, polygons and annotations with associated codification simply by picking with the mouse or digital pen into the SI window; these entities are directly geo-referenced in the 3D mapping coordinate system using the range matrix and the external orientation parameters of the SI.

In order to save the height information, it is possible to use a simple model of the local geoid (a plane) that defines local geoid height; this model is useful for correcting the ellipsoid height defined by the GNSS receiver into orthometric height.

The case study

The GSTOP application has been tested by producing a digital map of the Quaternary sediments and landforms in a sector of the alpine Rodoretto Valley (Fig. 8), a tributary of the Germanasca Valley (northwestern Italy).

The Germanasca Valley is located along the north-south tectonic thrust between the Dora Maira Massif, which outcrops on the valley's right side and the Greenstone and Schist Complex visible on the left side [Sandrone et al., 1993; Compagnoni and Hirajima, 2001]. These nappe systems include the Penninic Domain (Lower, Medium and Upper Penninic units) and the Piedmont Zone [Compagnoni, 2003].
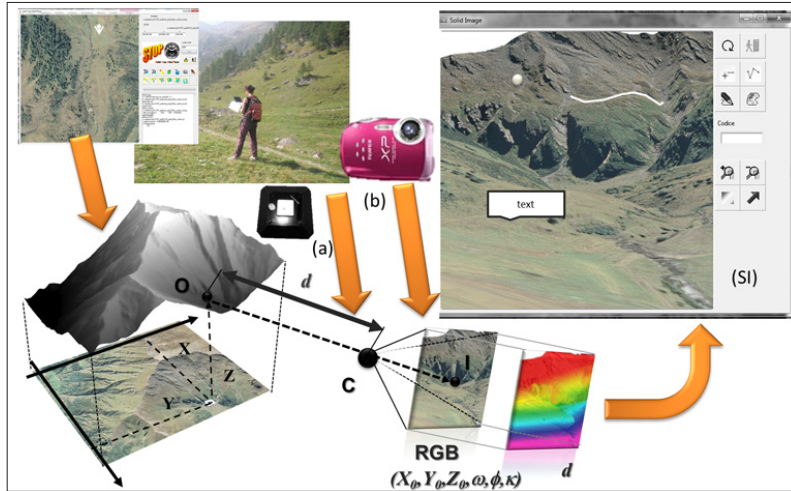
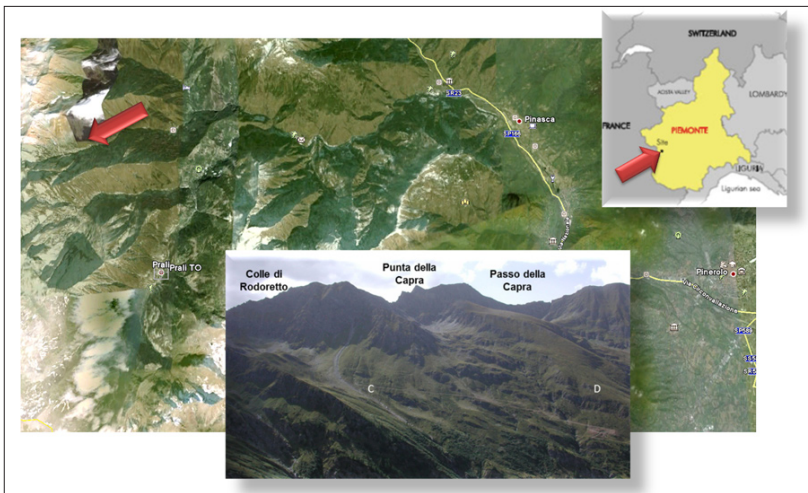**Figure 7 - The generation of SI using STOP data (b) with and (a) without additional digital camera.**

Figure 8 - The location of Rodoretto Valley (the case study).

The Dora Maira Massif is essentially constituted of garnet micaschists with chloritoid and blue-green amphiboles. The Greenstone and Schist Complex is a metamorphic system with Jurassic marine protolith sediments. The more diffuse lithotypes are schist, quartz schist, prasinite and serpentinite [Borghi et al., 1984]. The landforms and surficial sediments in this valley have resulted from the combinate effects of the Quaternary alpine glacial phases and deep-seated gravitative slope deformations. Therefore, the production of the geomorphological map has been focused on the relationships among landforms and sedimentary bodies developed during this period of the valley's evolution.
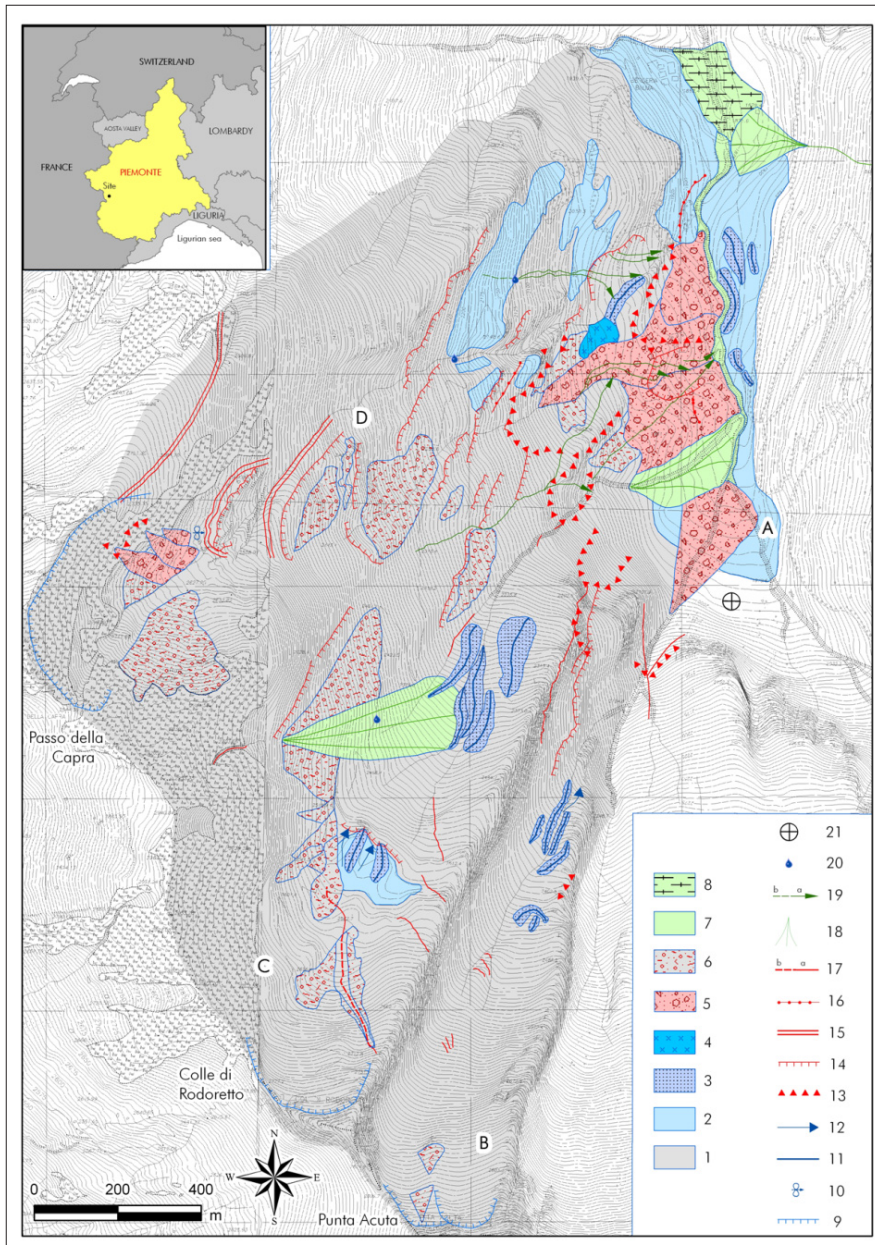
Figure 9 - Quaternary map of the Rodoretto Valley in the Germanasca Valley. 1: bedrock (greenstone schist complex); 2: subglacial sediments; 3: glacial till; 4: landslide main bodies; 5: rockfall main bodies; 6: debris flow and avalanche sediments; 7: lacustrine sediments; 8: glacial cirques; 9: roches moutonnées; 10: moraines; 11: glacial spillway channels; 12: landslide crowns; 13: minor scarps; 14: deep-seated gravitational slope doubled ridges; 15: linear trenches; 16: open tension cracks ((a) principal, (b) minor); 17: alluvial and avalanche fans; 18: palaeochannels ((a) principal, (b) minor); 19: groundwater springs; 20: geographical reference point; A, B, C, D: sectors [Forno et al., 2011].

The STOP of this area was produced using the following data provided by the government of Turin Province:

1) a true orthophoto with ground sample distance (GSD) of 50 cm generated from a set of images acquired by a digital aerial mapping camera (DMC by Zeiss/Intergraph);

2) a DDSM with 1 m GSD generated from aerial LiDAR data (2 points/m²) by means of geometric regularisation, filtering and resampling. With these data, no further (expensive) data acquisition operations have been required but the obtained representation is only in 2.5D. A professional user skilled in geomatics produced the STOP in 2 h.

Figures 10 and 11 show some occurrences that surveyors identified and recorded in an SI view generated using GSTOP, during field reconnaissance. On the right side, these features have been directly located into the GIS geomorphologic map with correct codes and symbolisation types.
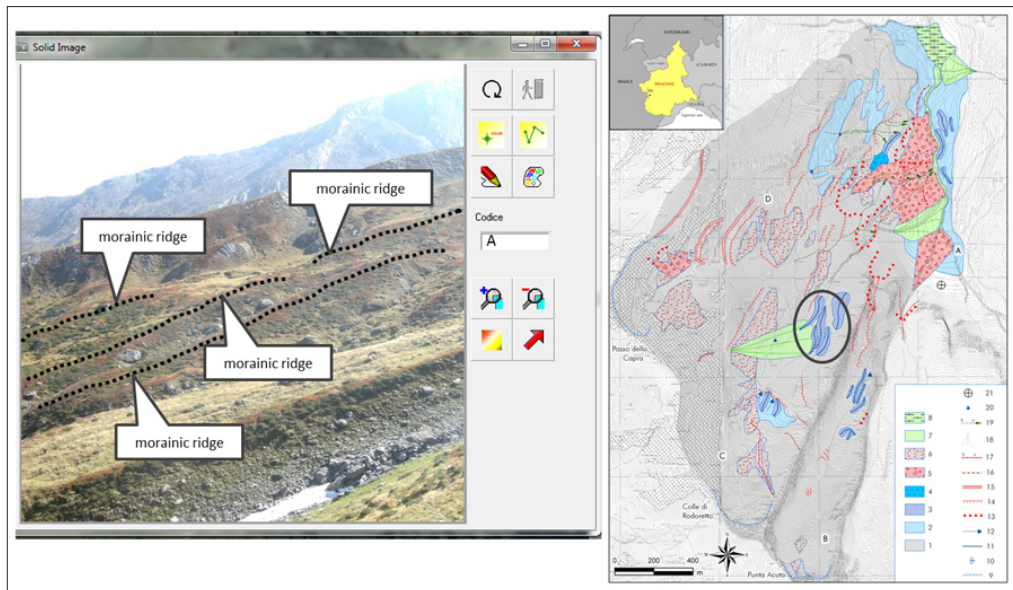

Figure 10 - The SI viewer generated by GSTOP to record some moraines.

Analysis of obtained accuracy/precision

The accuracy/precision of data extracted using GSTOP has not been defined for general cases because:

1) the GSTOP is an idea that can be realised in various ways: you can use different types of GNSS/IMU sensors to obtain different accuracy/precision of navigation data and therefore, different accuracy/precision of extracted data;

2) the quality (Ground Sample Density/Accuracy) of available data (DSM/DTM and orthophotos) substantially influences the final accuracy of the collected data.

Using the sensors described earlier, the nominal accuracy of this solution is about 2 m (4 m of tolerance) with:

1) a GPS position defined from EGNOS-WASS differential correction for a sub-metrical accuracy;

2) an accuracy of 1 gon of attitude angles;
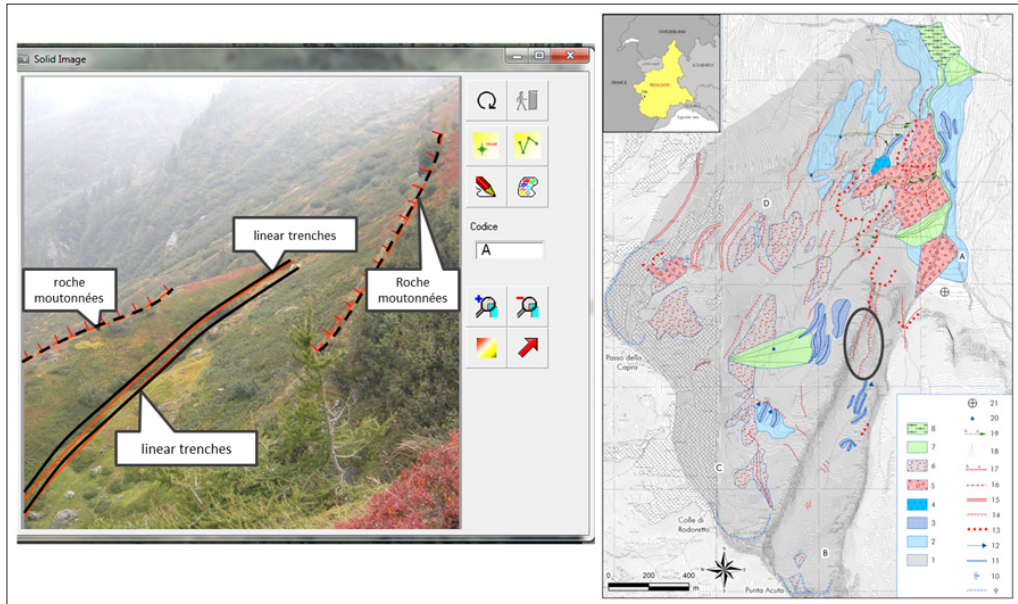3) the distance from object is limited to 100 m.

Figure 11 - The SI viewer generated by GSTOP to acquire linear trenches and roches moutonnées.

The practical definition of the accuracy/precision of GSTOP has been performed only for the described configuration of GNSS/IMU sensors and the specific quality of available data (DTM/orthophotos in nominal scale 1:5000).

A specific procedure of in field survey has been realised to obtain a comparison set of correct data; several geodetic details collected by GSTOP have been surveyed using geodetic GNSS receivers in RTK (Real Time Kinematic) configuration connected to the GNSS permanent network of the Piedmont region. As is well known, this positioning technique ensures an accuracy of about 1-2 cm for planimetric coordinates (x, y) and 5 cm for the altimetric component (z). The discrepancies (Δx, Δy, Δz) from the coordinates acquired by RTK/GNSS and the coordinates of the corresponding details acquired by GSTOP have been determined, as shown in Figure 12.

Statistical parameters of these discrepancies (Tab. 1) demonstrate that the data collected by GSTOP are practically coherent with the precision/tolerance of a digital map of a nominal scale 1:10000, without significant systematic errors.

About 100 dips and directions estimated using GSTOP have been compared with the relative values obtained by manual surveys using a geological compass with an inclinometer. The compass bearing has been corrected using local magnetic declination and local convergence of the meridian. The angular discrepancies have been calculated to evaluate the accuracy of dips (rms = 3.125 gons) and directions (rms = 3.214 gons). The results are comparable with similar low cost instruments for navigation purposes, in accordance with [Guarnieri et al., 2011].
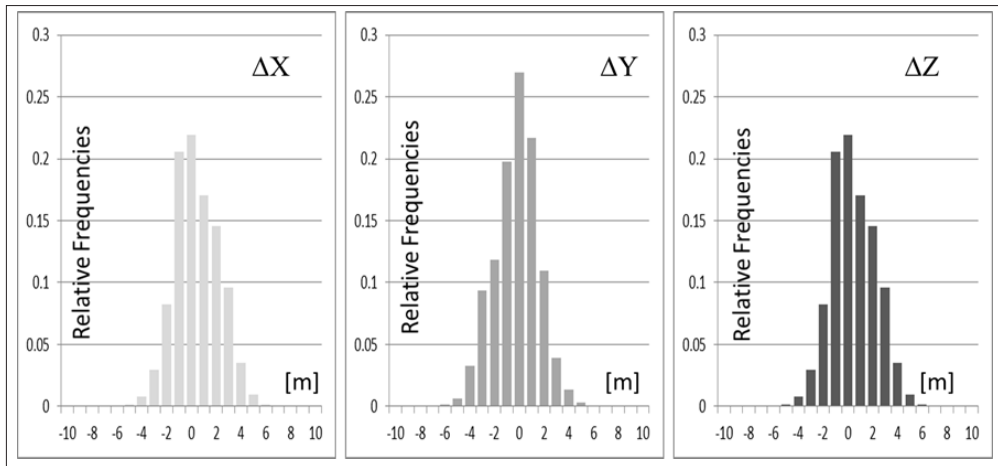
Figure 12 - Distributions of discrepancies.

Table 1 - Statistical parameters of discrepancies.

	Δx [m]	Δy [m]	Δz [m]
Mean	0.45	-0.23	1.08
Dev.st.	1.80	1.78	2.86
Min	-6.30	-9.50	-10.70
Max	7.50	8.50	9.55
Min (95%)	-3.95	-3.87	-4.23
Max (95%)	3.76	3.92	4.65

Conclusions

A new, detailed geomorphological map of the Rodoretto Valley Quaternary cover has been produced. The investigation recorded previously unmapped glacial tributary evidence, such as lateral and frontal moraines and outwash incisions connected to small local Pleistocene glaciers. A wide, deep-seated gravitational slope deformation has been also defined, forming many trenches of various sizes, doubled ridges and slide scarps.

Geologists unskilled in geomatics have efficiently used the STOP viewer on a Tablet PC during field surveys. The 3D visualisation tools offered by the STOP viewer software have facilitated the immediate interpretation of relict landforms with:

1) time savings during acquisition and loading into GIS software;

2) minor number of blunders that limits repeated reconnaissance and accelerates map productions;

3) better understanding of the morphological evidence with the availability of 3D geometric information integrated with 2D views similar to what the surveyor sees.

The future development of the system involves its implementation in multiplatform smartphones, tablet PC and iPAD using lighter and precise GNSS/IMU sensors that microelectronic technology is developing.

References

Athey J.E., Freeman L.K., Woods K.A. (2008) - *The transition from traditional to digital mapping: maintaining data quality while increasing geologic mapping efficiency in Alaska*. Alaska GeoSurvey News, 11 (2): 1-11.

Barnes J., Lisle R. (2004) - *Basic Geological Mapping*. John Wiley & Sons Ltd., 204: 10-12.

Biasion A., Bornaz L., Rinaudo F. (2005) - *Laser Scanning Applications on Disaster Management*. In "Geo-information for Disaster Management", Van Oosterom P., Zlatanova S., Fendel E. (Editors), Springler: 19-34. doi: http://dx.doi.org/10.1007/3-540-27468-5_2.

Borghi A., Cadoppi P., Porro A., Sacchi R., Sandrone R. (1984) - *Osservazioni geologiche nella Val Germanasca e nella media Val Chisone (Alpi Cozie)*. Boll. Mus. Reg. Sc. Nat. Torino, 2 (2): 503-526.

Bornaz L., Dequal S. (2003) - *A new concept: the solid image*. CIPA 2003 Proceedings of XIXth International Symposium: 169-174.

Brimhall G.H., Vanegas A., Lerch. D. (2002) - *Geomapper Program for Paperless Field Mapping with Seamless Map Production in ESRI ArcMap and GeoLogger for Drill-Hole Data Capture: Applications in Geology, Astronomy, Environmental Remediation, and Raised-Relief Models, in Digital Mapping Techniques '02* - Workshop Proceedings (Soller D.R., editor). U.S. Geological Survey Open-file Report, 370: 141-152.

Brodaric B. (1997) - *Field Data Capture and Manipulation using GSC FIELDLOG v3.0, in Proceedings of a Workshop on digital mapping techniques: methods for geologic map capture, management, and publication*. U.S. Geological Survey Open-file Report, 269: 77-81.

Brown K.D., Sprinkel D.A. (2008) - *Geologic field mapping using a rugged tablet computer*. U.S. Geological Survey Open-File Report, 1385: 53-58.

Clegg P., Bruciatelli L., Domingos L., Jones R.R., De Donatis M., Wilson R.W. (2006) - *Digital geological mapping with tablet PC and PDA: A comparison*. Computers & Geosciences, 32: 1682-1698. doi: http://dx.doi.org/10.1016/j.cageo.2006.03.007.

Compagnoni R. (2003) - *HP metamorphic belt of the western Alps*. Episodes, 26 (3): 200-204.

Compagnoni R., Hirajima T. (2001) - *Superzoned garnets in the coesite bearing Brossasco-Inasca Unit, Dora Maira massif, Western Alps, and the origin of the whiteschists*. Lithos, 57: 219-236. doi: http://dx.doi.org/10.1016/S0024-4937(01)00041-X.

De Agostino M., Lingua A., Piras M. (2012) – *Rock face surveys using a LiDAR MMS*. European Journal of Remote Sensing, 44: 141-151.

De Donatis M., Bruciatelli L., Susini S. (2005) - *MAP IT: A GIS/GPS software solution for digital mapping, in digital mapping techniques '05* - Workshop proceedings (Soller D.R., editor): U.S. Geological Survey Open-file Report, 1428: 97-101.

Dequal S., Lingua A. (2003) - *True orthophoto of the whole town of Turin*. Int. Arch Photogramm. Remote Sens., 34 (5/C15:263– 268): 1682-1750.

Edmondo G.P. (2002) - *Digital Geologic Field Mapping using ArcPad, in Digital Mapping Techniques '02* - Workshop Proceedings (Soller D.R., editor): U.S. Geological Survey Open-file Report, 370: 129-134.

Forno M.G., Lingua A., Lo Russo S., Taddia G. (2011) - I*mproving digital tools for Quaternary field survey: a case study of the Rodoretto Valley (NW Italy)*. Environmental Earth Sciences, 64: 1487-1495. doi: http://dx.doi.org/10.1007/s12665-011-0971-6.

Guarnieri A., Milan N., Pirotti F., Vettore A. (2011) - *Motion estimation by integrated*

low cost system (Vision and MEMS) for positioning of a scooter "vespa". Proc. of 7th Symposium on Mobile Mapping Technology, Cracovia (Poland). In Archives of Photogrammetry, Cartography and Remote Sensing, 22: 147-158.

Jones R.R., McCaffrey K.J.W., Wilson R.W., Holdsworth R.E. (2004) - *Digital field acquisition: towards increased quantification of uncertainty during geological mapping*. In: Curtis A., Wood R. (Editors.), Geological Prior Information, Geological Society of London, Special Publication, 239: 43-56.

Kraus K. (1997) - *Photogrammetry, Advanced Methods and Applications*. Reading: Dümmlers Verlag, 2: 2-285.

McCaffrey K.J.W., Jones R.R., Holdsworth R.E., Wilson R.W., Clegg P., Imber J., Holliman N., Trinks I. (2005) - *Unlocking the spatial dimension: digital technologies and the future of geoscience fieldwork*. Journal of the Geological Society, London, 162: 927-938. doi: http://dx.doi.org/10.1144/0016-764905-017.

McGlone J.C., Mikhail E.M., Bethel J.B., Mullen R. (2004) - *Manual of Photogrammetry* - Fifth Edition, American Society of Photogrammetry and Remote Sensing: 648-668.

Pirotti F., Grigolato S., Lingua E., Sitzia T., Tarolli P. (2012) - *Laser Scanner Applications in Forest and Environmental Sciences*. Italian Journal of Remote Sensing 44 (1), 109-123. doi: http://dx.doi.org/10.5721/ItJRS20124419.

Sandrone R, Cadoppi P, Sacchi R, Vialon P. (1993) - *Pre-mesozoic geology in the Alps*. In: Von Raumer JF, Neubaur F (editors) The Dora-Maira Massif. Springer Verlag, Berlin: 45-61.

Sprinkel D.A., Brown K.D. (2008) - *Using Digital Technology in the Field*. Utah Geological Survey, Survey Notes, 40 (1): 1-2.

Walsh G.J., Reddy J.E., Armstrong T.R. (1999) - *Geologic Mapping and Collection of Geologic Structure Data with a GPS Receiver and a Personal Digital Assistance (PDA) Computer*. in Digital Mapping Techniques '99 - Workshop Proceedings Soller D.R. (editor): U.S. Geological Survey Open-file Report, 386: 127-131.

Wilson R.W., McCaffrey K.J.W., Jones R.R., Clegg P., Holdsworth R.E. (2005) - *Digital mapping of Lofoten's faults*. Geoscientist, 15: 2.